Platelet microparticle membranes have 50- to 100-fold higher specific procoagulant activity than activated platelets

Elena I. Sinauridze[1], Dmitry A. Kireev[1], Nadezhda Y. Popenko[1], Aleksei V. Pichugin[2], Mikhail A. Panteleev[1], Olga V. Krymskaya[1], Fazoil I. Ataullakhanov[1,3,4]

[1]National Research Center for Hematology, Russian Academy of Medical Sciences, Moscow, Russia; [2]Institute of Immunology, Ministry of Health, Moscow, Russia; [3]Faculty of Physics, Moscow State University, Moscow, Russia; [4]Center for Theoretical Problems of Physicochemical Pharmacology, Russian Academy of Sciences, Moscow, Russia

Summary

Platelet microparticles (PMPs) are small vesicles released from blood platelets upon activation. The procoagulant activity of PMPs has been previously mainly characterized by their ability to bind coagulation factors VIII and Va in reconstructed systems. It can be supposed that PMPs can contribute to the development of thrombotic complications in the pathologic states associated with the increase of their blood concentration. In this study, we compared procoagulant properties of calcium ionophore A23187-activated platelets and PMPs using several in-vitro models of hemostasis. Surface densities of phosphatidylserine, CD61, CD62P and factor X bound per surface area unit were determined by flow cytometry. They were 2.7-, 8.4-, 4.3-, and 13-fold higher for PMPs than for activated platelets, respectively. Spatial clot growth rate (V_{clot}) in the reaction-diffusion experimental model and endogenous thrombin potential (ETP) were determined in plasma, which was depleted of phospholipid cell surfaces by ultra-centrifugation and supplemented with activated platelets or PMPs at different concentrations. Both V_{clot} and ETP rapidly increased with the increase of PMP or platelet concentration until saturation was reached. The plateau values of V_{clot} and ETP for activated platelets and PMPs were similar. In both assays, the procoagulant activity of one PMP was almost equal to that of one activated platelet despite at least two-orders-of-magnitude difference in their surface areas. This suggests that the PMP surface is approximately 50- to 100-fold more procoagulant than the surface of activated platelets.

Keywords

Platelet, PMPs, procoagulant activity, spatial dynamics of coagulation, thrombin generation, factor X, phosphatidylserine, CD-61, CD-62P

Thromb Haemost 2007; 97: 425–434

Introduction

The system of blood coagulation is a complex reaction cascade with numerous positive and negative feedback loops (1). Not only plasma proteins, but also vessel wall and blood cells play important roles in the clotting process. Among blood cells, platelets are assumed to be the most important for coagulation. One consequence of platelet activation is the exposure of phosphatidylserine (PS) in the outer leaflet of the platelet membrane (2). The tenase and prothrombinase procoagulant complexes assemble on this negatively charged phospholipid surface. These complexes play a critical role in the functioning of important positive feedbacks, which accelerate activation of factors X and II, respectively, by several orders of magnitude (3). Another important result of platelet activation is shedding of small vesicles, or microparticles, from the platelet membrane (4, 5).

An increasing number of studies were recently focused on the investigation of microparticles formed from various cells of blood and vascular wall (6–8) and on the analysis of their origin, composition, and possible function. It has been shown that increased blood microparticle concentration is associated with such pathological states as severe trauma, cardiovascular diseases, etc. (9–11). Cell-derived microparticles were also detected in the blood of healthy donors, and almost half of them were of platelet origin (12).

Correspondence to:
E. I. Sinauridze
National Research Center for Hematology
Russian Academy of Medical Sciences
4a Novyi Zykovskii proezd, Moscow 125167, Russia
Tel.: +7 495 612 8870, Fax: +7 495 612 8870
E-mail: helen@blood.ru

Financial support:
This study was supported in part by grant 06–04–48426 from the Russian Foundation for Basic Research and by Russian Federation President Grant for Young Candidates of Science MK-7062.2006.4 from the Federal Agency of Science and Innovations.

Received June 7, 2006
Accepted after resubmission January 9, 2007

Prepublished online February 8, 2007
doi:10.1160/TH06–06–0313

Several works showed that platelet-derived microparticles (PMPs) formed during platelet activation are procoagulant (9, 12–16). The principal lines of evidence are the following. i) PMPs are formed by platelets upon activation, and hence their membrane should possess all properties of the activated platelet membrane (13, 14); ii) PMPs can bind components of procoagulant complexes such as factors V(Va) and VIII(VIIIa); moreover, the binding-site densities for these proteins on PMP membranes even exceed those on platelet membranes (15, 16); iii) Addition of PMPs to platelet-free recalcified plasma without added coagulation activators accelerates initiation of thrombin generation (9, 12).

However, numbers of binding sites for factors Va and VIII were determined in washed platelet or PMP suspensions in the presence of excess coagulation factor concentrations, which were significantly above their physiological values. In addition, PMP membranes are known to enhance not only the prothrombinase and tenase formation, but their inhibition as well (17). Therefore, these data can only indirectly predict the effect of PMPs on coagulation in plasma under physiological conditions. Existing thrombin generation studies (9–12) reported only the initial reaction stage (first 15 minutes [min]) in recalcified plasma without added tissue factor. Absence of the complete curve and physiological activation in these experiments does not allow making a conclusion about the overall PMPs effect on coagulation.

The objective of this study was to compare directly the effects of activated platelets and of PMPs on plasma coagulation using two in-vitro models of hemostasis/thrombosis: thrombin generation assay (18) and spatial clot formation in non-stirred plasma (19–21). In the former method, the activator is uniformly distributed over the reaction volume. On the other hand, studies of the spatial clotting dynamics in non-stirred plasma allow separate determination of the different parameters' effects on the initiation and propagation phases of clot formation. In addition, size of PMPs, quality of their isolation from platelets, and their ability to bind activation markers and coagulation factors were characterized by flow cytometry.

The principal conclusion of this study is that abilities of an activated platelet and a PMP to support coagulation are very similar. Taking into account an approximately 100-fold difference in their surface area, it can be concluded that specific procoagulant activity of the PMP membranes is approximately 50- to 100-fold higher than that of activated platelets. Most likely, this occurs, because phosphatidylserine and membrane proteins participating in the coagulation factors binding are concentrated on PMPs during the shedding process.

Materials and methods

Materials

Calcium ionophore A23187, $CaCl_2$, bovine serum albumin (BSA), apyrase grade VII from potato and Quantum Fluorescent Microbead Standard for fluorescein were from Sigma (St. Louis, MO, USA). FluoReporter Fluorescein-EX Protein Labeling Kit and annexin V-FITC conjugate were from Molecular Probes (Eugene, OR, USA). Ethylene diamine tetraacetic acid disodium salt (EDTA) was from SERVA, Feinbiochemica (Heidelberg, Germany). 4-(2-hydroxyethyl)-1-piperazine-2-ethanesulfonic acid (HEPES) was from Fisher Biotech (Fair Lawn, NJ, USA). Kaolin was from Boehringer Mannheim GmbH (Mannheim, Germany). Prostaglandin E1 was from MP Biochemicals (Irvine, CA, USA).

The following monoclonal antibodies were used in this study: mouse anti-human CD61 labeled with peridinin-chlorophyll-protein complex (anti-CD61-PerCP), clone RUU-PL7F12 (Beckton Dickinson Biosciences, San Jose, CA, USA), mouse anti-human CD62P antibodies labeled with phycoerythrin (anti-CD62P-PE), clone AK-4 (eBioscience, San Diego, CA, USA), control mouse IgG_1-PerCP γ_1, clone X40 and control mouse $IgG_1/IgG_{2\alpha}$-FITC/PE γ_1/γ_2 Simultest^{TM} IMK, clone X40/X39 (Beckton Dickinson Bioscience).

Human fetal lung fibroblast line was from the Ivanovskii Research Institute of Virology (Russian Academy of Medical Sciences, Moscow, Russia). Cells (10^3 cells/ml) were grown for two days on poly(ethylene terephthalate) film slips (Joint Institute for Nuclear Research, Dubna, Moscow Region, Russia) as described previously (19).

Thrombin-specific fluorogenic substrate BOC-Ile-Gly-Arg-AMC (22), where BOC is the tret-butoxycarbonyl residue and AMC is the 7-amino-4-methylcoumarine residue, was synthesized in the Institute for Medical and Biological Chemistry (Moscow, Russia). The working substrate solution (5 mM) was prepared by dissolving the substrate in dimethylsulfoxide (DMSO, 1/4 v/v) and adding of 3/4 v/v buffer (145 mM NaCl, 20 mM HEPES, pH 7.5). The calibration solution of AMC (100 μM) was prepared in dimethylsulfoxide (DMSO). Both solutions were stored at –32ºC. Calibration beads (Level II, Med-low, 5 μm diameter) were obtained from Epics Division of Coulter Corporation (Hialeah, FL, USA). Calibration beads with different diameters (Fluoresbrite® Carboxylate Size Range Kits I and II) were from Polysciences Inc. (Warrington, PA, USA). Human factor X and prothrombin were from Enzyme Research Laboratories (South Bend, IN, USA). Coagulo-test kit and thromboplastin for activated partial thromboplastin time (APTT), prothrombin time (PT), and kaolin time (KT) measurements were from Renam (Moscow, Russia). All other chemicals were of reagent and analytical grade.

Blood collection and platelet-free plasma (PFP) preparation

Donor blood was collected into 3.8% sodium citrate (pH 5.5) with a blood/anticoagulant ratio of 9/1. To prepare PFP, blood was centrifuged for 15 min at 1,500 g followed by additional centrifugation of the supernatant for 10 min at 10,000 g. The pH value of the platelet-free plasma was stabilized at 7.2–7.6 by lactic acid treatment (23).

Ultra-free plasma (UFP) preparation and characterization

To obtain plasma depleted of cells, microvesicles, and cell membrane remnants, which can provide procoagulant surface for the assembly of the tenase and prothrombinase complexes, PFP was ultra-centrifuged at 100,000 g for 1 hour (h) at 21°C as described earlier (21, 24, 25). Our estimations based on (26) showed that no significant sedimentation of coagulation protein molecules (in-

cluding the factor VIII-von Willebrand factor complexes, which can reach a Mr of 2–2.5x10^6 D) could occur at these centrifugation conditions. Coagulation parameters of UFP were characterized by standard clotting assays: APTT, PT and KT, and by determination of the spatial clot growth rate. APTT and PT for the studied UFP were within the range of normal values (data not shown). Concentration of exogenous procoagulant lipids added in these tests is very high, so their depletion should not affect the tests results. On the other hand, in the tests without addition of exogenous procoagulant lipids (KT and spatial clot growth model), clotting was delayed. KT was elongated five- to nine-fold, and clot growth rate was decreased four-fold, indicating that the concentration of procoagulant surfaces was significantly reduced in UFP.

Fluorescence labeling of factor X

For binding experiments, factor X was labeled with fluorescein using FluoReporter Fluorescein-EX Protein Labeling Kit (Molecular Probes) as described (27). The degree of labeling was determined by absorbance at 280 and 494 nm and was 2.8 molecules of dye per molecule of factor X. The protein was stored at –80°C in small aliquots (5–10 μl) and thawed only once before use.

Isolation of platelets and preparation of activated platelets and PMPs

Platelets were obtained from healthy donor venous blood as described (28) with some modifications. Prostaglandin E1 (1 μM) and apyrase (0.1 unit/ml) were added in whole blood to prevent activation, and blood was centrifuged at 100 g for 10 min. Platelet-rich plasma (PRP) was collected as supernatant, and its pH was set to 6.5 with 3.8% sodium citrate (pH 5.0). Platelets were sedimented by centrifugation at 350 g for 15 min. After removal of supernatant, platelets were washed by centrifugation at 350 g for 15 min with a buffer containing 145 mM NaCl, 2.7 mM KCl, 10 mM HEPES, 0.1% BSA, pH 6.5 (buffer A) and resuspended in the same buffer with pH 7.4 (buffer B). To prepare PMPs, platelet concentration was adjusted by buffer B to 2.0–3.0 X 10^5 per μl as determined by blood cell counter (Beckman Coulter). Platelets were activated by calcium ionophore A23187 (10 μM) for 15 min at 37°C (14) and then sedimented by centrifugation at 350 g for 15 min. The supernatant was collected and additionally centrifuged at 16,000 g for 30 min. Sedimented microparticles were washed once and resuspended in buffer B. The concentration of platelets in PMP preparations was below the detection limit of the cell counter (~10^3 platelets/μl, i.e. below 1%). Platelets sedimented after the activation were washed once with buffer A, and resuspended in buffer B to obtain activated platelets. Those preparations contained 2–5% of PMPs as estimated by flow cytometry.

Microparticle concentration was calculated using flow cytometer by comparison with known concentration of 5 μm diameter calibration beads added to every sample (10 μl of 10^6/ml suspension per 300 μl sample). The sample was analyzed until 200 calibration beads were counted. The concentration of PMPs in the sample was calculated using the number of PMPs counted and the known concentration of calibration beads.

Flow cytometry

All samples were analyzed in a Becton Dickinson FACSCalibur flow cytometer (San Jose, CA, USA) with CellQuest software (Becton Dickinson) as described (29, 30) with some modifications. The flow cytometer was formatted for three-color analysis. Light scatter and fluorescence channels were set at logarithmic gain. Platelets and PMPs are significantly different in size and thus could be identified by their light scatter as distinct regions in the forward scatter (FSC) versus sideward scatter (SSC) dot plots (Fig. 1A). To differentiate platelets and PMPs from background light scatter, acquisition was gated so as to include only the particles distinctly positive for anti-CD61-PerCP. Fluorescence threshold on the 680 nm channel was set to exclude background scatter and auto fluorescence of unlabeled particles. By this method, only particles expressing platelet-specific CD61 were included for analysis. Each sample was analyzed for FSC, SSC, and for FITC, phycoerythrin and PerCP fluorescence intensities.

Washed platelets, activated platelets, or PMPs were diluted to the concentration of 2–3x10^5/μl with buffer B, which was ultracentrifuged beforehand at 100,000 g for 1 h. Aliquots of 5 μl of each suspension were added to 40 μl of the same buffer containing additionally $CaCl_2$ (2.5 mM). To this mixture, 5 μl anti-CD61-PerCP, 5 μl anti-CD62P-PE, and 5 μl annexin V-FITC were added followed by incubation for 20 min at room temperature in the dark. The reactions were stopped by samples dilution with 300 μl of the same buffer, and the samples were immediately analyzed by flow cytometry. All data were corrected using isotype and auto fluorescence controls.

Acquired data were analyzed using WinMDI 2.8 software (Joseph Trotter, Scripps Research Institute, La Jolla, CA, USA). To obtain either size or fluorescence density per surface area unit distributions, the experimental parameters were re-calculated using Flow Explorer 4.1 (Ron Hoebe, University of Amsterdam, The Netherlands). Size of cells and PMPs was calculated using a calibration curve obtained with Fluoresbrite beads of different diameters (0.1–5 μm).

Factor X binding experiments

To study factor X binding to platelets, activated platelets or PMPs, FITC-labeled factor X (6 μl, 1.8 μM), platelets or PMPs (5 μl, 2–2.5×10^5/μl), and anti-CD61-PerCP (5 μl) were incubated in buffer B supplemented with 2.5 mM $CaCl_2$ (44 μl), for 20 min in the dark. The final concentration of factor X-FITC was 180 nM. The mixture was quickly diluted with 300 μl of the same buffer containing 2.5 mM $CaCl_2$, and the count was run immediately. Mean fluorescence intensity of platelet-bound factor X was determined. Calcium-independent binding was subtracted using experiments with buffer containing 10 mM EDTA instead of $CaCl_2$ as the controls. The mean fluorescence intensity was converted to the number of bound factor X molecules using a calibration curve prepared with Quantum Fluorescent Microbead Standard with known numbers of FITC molecules per bead. Control kinetic experiments confirmed that factor X dissociation from platelets caused by the sample dilution was negligible during the time of analysis (data not shown).

Spatial clot growth

Spatial parameters of clot formation were studied using a light scattering and video microscopy recording system (19, 20). The microchamber was assembled in a 35-mm polystyrene Petri dish around a 1 mm-thick microscope glass slide fixed to its bottom. The glass slide edge, which formed a vertical wall of a chamber, was wrapped around with a cell-coated poly(ethylene terephthalate) slip. The microchamber was covered with a piece of black polystyrene which formed the upper surface. Recalcified (20 mM final concentration of added $CaCl_2$) human plasma was transferred into the assembled chamber. The dish was sealed and placed in a temperature-controlled water jacket (37ºC). The microchamber was illuminated from below with red light emitting diodes (peak wave length 660 nm), and the light-scattering image from a 7.2 x 5.4-mm area of microchamber was monitored by OS-75D camera (Mintron Enterprise, Taiwan) coupled to EZ98 frame grabber (Lifeview Inc., Fremont, CA, USA).

Image processing

Parameters of spatial clot formation were determined from the experimental image series as described in (19, 20). Briefly, a tissue-factor-bearing cell monolayer initiated clotting, which spread from its surface into plasma. V_{clot} was characterized by the rate at which the fibrin clot extended away from the cell monolayer. For every frame, the clot size was determined as a distance between the initiator cell surface and the clot edge defined as a point where the light scattering intensity was half-maximum. V_{clot} was derived from the clot size versus time curve as a mean rate in the range of 10–35 min following the onset of clotting.

Thrombin generation assay

Thrombin generation assay was performed according to the basic method of (18) with minor modifications. To the wells of 96-well flat bottom plate, we added 90 µl of citrate plasma (PFP or UFP), 10 µl of platelets or PMPs suspension, and 20 µl of slow fluorogenic substrate BOC-Ile-Gly-Arg-AMC (5 mM). The mixture was incubated for 10 min at 37°C. Coagulation was triggered simultaneously in all wells by addition of 25 µl of activator in buffer B containing 80 mM $CaCl_2$ (pH 7.5). As activators, 400-fold diluted rabbit thromboplastin solution (PT reagent, Renam, Moscow, Russia) or 50-fold diluted kaolin suspension (APTT reagent, Boehringer Mannheim, Germany) were used. Final concentrations of tissue factor or kaolin were 4 pM as determined using Actichrome® TF chromogenic activity assay (American Diagnostica, Stamford, CT, USA) or 0.02 mg/ml, respectively. AMC fluorescence was monitored continuously for 45–50 min using fluorimetric Fluoroscan II reader (LabSystem, Finland) at λ_{ex}=380 nm and λ_{em}=440 nm. Each specimen was reproduced in triplicates, and the mean fluorescence value was used. The data were processed using Origin 6.0 software (Microcal Software, Northampton, MA, USA). Fluorescence intensity was corrected for α_2-macroglobulin-thrombin complex activity using a specially written program. Fluorescence was converted to AMC concentration with the help of a calibration determined individually for each sample by measuring fluorescence of a known AMC concentration added to the same plasma with the same platelet/PMP and substrate concentrations. Linearity of the calibration curve under a wide range of conditions was confirmed in separate experiments (data not shown). From the thrombin generation curve, total area under curve (endogenous thrombin potential [ETP]) was determined.

Results

Flow cytometry characterization of the intact and activated platelets and PMPs

The size and the state of the studied cells and membrane particles were characterized using flow cytometry. Their light scattering and expression of general platelet marker CD 61 and activation markers phosphatidylserine (PS) and P-selectin (CD 62P) were determined.

Activated platelets and PMPs significantly differ in their size. This allows their separation by the light scattering in the two-dimensional FSC versus SSC flow cytometry dot plots. Figure 1A shows a typical dot plot for a mixture of activated platelets and PMPs: platelets can be distinctly seen in the upper right region (P), and PMPs are in the lower left region (V).

To compare specific procoagulant activity of activated platelet and PMP surface, it is essential to estimate their surface

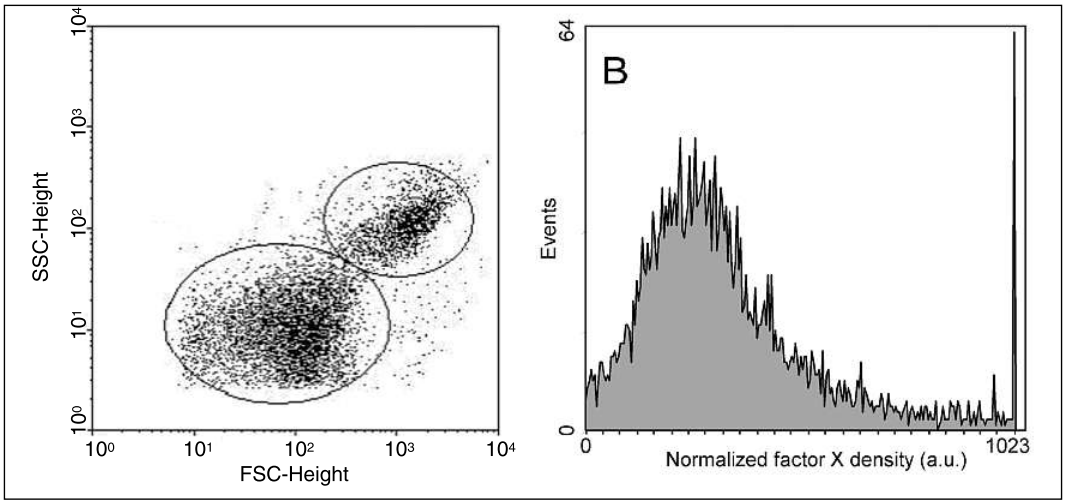

Figure 1: Flow cytometry analysis of platelets and PMPs. A) Typical dot plot of forward light scatter (FSC) versus sideward light scatter (SSC) for a suspension containing activated platelets (region P) and PMPs (region V). B) Typical distribution of the bound factor X density per surface unit on activated platelets. The distribution was obtained from the FSC and fluorescence data with the help of Flow Explorer 4.1 software (Ron Hoebe, University of Amsterdam, The Netherlands) using formulas 1 and 2.

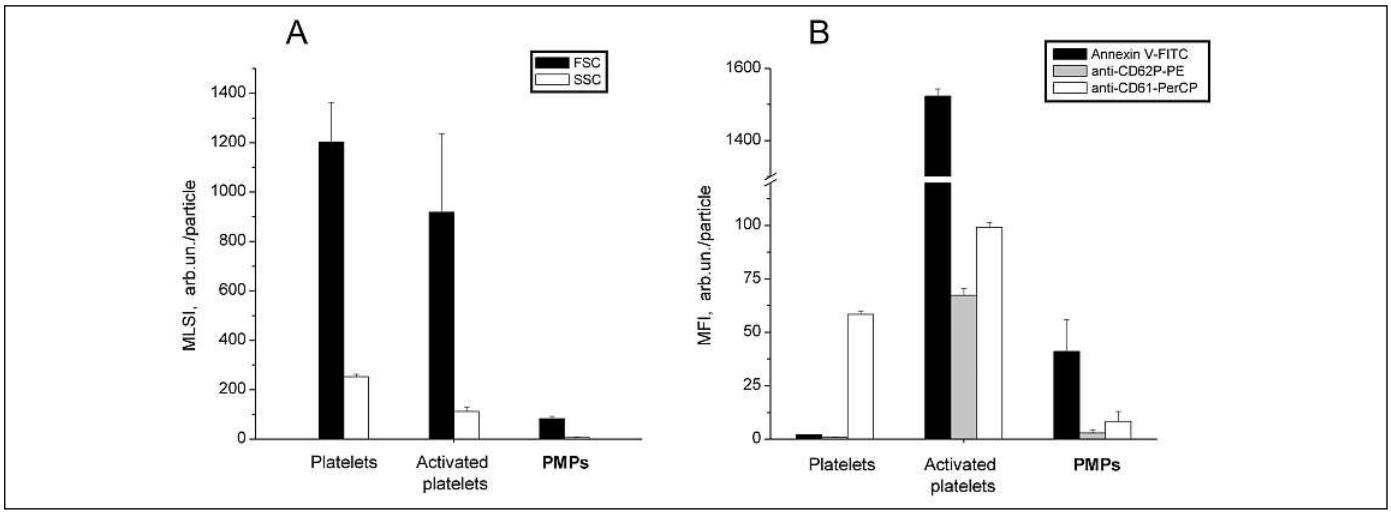

Figure 2: Mean light scatter (A) and mean fluorescence intensity of annexin V-FITC, anti-CD61-PerCP, or anti-CD62P-PE (B) per cell/particle in the suspensions of intact platelets, activated platelets and PMPs. For each sample, 5 µl of the suspension containing platelets or PMPs at 2–3x10^5 per µl was added to 40 µl of buffer B containing 2.5 mM $CaCl_2$, followed by addition of 5 µl FITC-labeled annexin V, anti-CD61-PerCP, and anti-CD62P-PE. The mixture was incubated in the dark at room temperature for 20 min. The samples were then diluted with 300 µl of the same buffer containing known concentration of 5 µm calibration beads and immediately analyzed on the flow cytometer formatted for three-color analysis.

areas correctly. For these experiments, these areas were calculated using a spherical model (31) and the FSC data. It is known that, within the micrometer range of sizes, it is a good approximation that FSC determined by the cytometer is an exponential function of the object size (15). We measured FSC for Fluoresbrite beads of five different diameters (0.1–5 µm) and fitted the obtained calibration curve using a linear model in a semi-logarithmic scale. The fitting allowed us to determine parameters and use the following connection between FSC and diameter (formula 1):

$$D = A \cdot \ln\left(\frac{FSC}{B}\right)$$

where D is diameter (in µm), and parameters are A=1.07 ± 0.18 µm, and B=64 ± 22 arb.un.

Using formula 1 and mean FSC values for activated platelets (827.11 ± 135.29 arb.un, n=5) and PMPs (FSC 84.03 ± 8.50 arb.un., n=7), we calculated mean diameters, which were 2.81 ± 0.18 and 0.29 ± 0.11 µm, respectively. The mean surface of activated platelet was approximately 95.4-fold greater that that of PMP. Diameter determined on the basis of FSC is only an estimate usually tending to exceed the real size (because surface and internal irregularities of cells and particles can increase the scatter) and should be used with caution. However, there is no doubt that diameters of platelets and PMPs in our experiments differ by approximately an order of magnitude meaning that their surfaces differ approximately 100-fold.

Then we used formula 1 and Flow Explorer 4.1 (Ron Hoebe, University of Amsterdam, The Netherlands) to recalculate experimental files and obtain normalized specific fluorescence intensity for each observed event according to formula 2:

$$F_{norm} = k \cdot \frac{F}{D^2}$$

where F_{norm} is the normalized specific fluorescence, F is fluorescence intensity, and k is a normalization coefficient (k=24). The obtained values were (with the coefficients) the distributions of all analyzed events by the densities of analyzed markers or factor X binding per surface area unit of the particle. This is illustrated by Figure 1B showing normalized density distribution (in the linear scale) of bound factor X for a typical experiment with activated platelets.

The mean light scatter intensity and fluorescence of different markers for intact and activated platelets and for PMPs are

Table 1: Mean fluorescence intensities (MFIs) of different platelet markers per 1 µm² of membrane for activated platelets and PMPs.

Particle parameter	PMP*) (n=7)	Activated platelet*) (n=5)	Ratio of the values PMP/Act. Plt.§)
Surface S (µm²)	0.26 (d=0.29 µm)	24.8 (d=2.81 µm)	0.01
MFI $_{Annexin\ V\text{-}FITC}$/S (arb.un./µm²)	158.2 ± 52.0	58.6 ± 1.9	2.7 (1.7–3.7)
MFI $_{CD62P\text{-}PE}$/S (arb.un./µm²)	11.2 ± 5.6	2.6 ± 1.1	4.3 (1.5–10.9)
MFI $_{CD61\text{-}PerCP}$/S (arb.un./µm²)	32.1 ± 16.2	3.8 ± 0.8	8.4 (3.5–15.7)

*) Mean values ± confidence intervals ($p<0.05$). §) Ratios of the mean values; the possible range of values is given in the parentheses.

Particle parameter	Platelet*) (n=3)	Activated platelet*) (n=3)	PMP*) (n=5)	Ratio of the values PMP/Act. plt.§)
$N_{FX\text{-}FITC}$ /particle (1/particle)	52 ± 160	3229 ± 606	422 ± 203	0.13 (0.06–0.24)
$N_{FX\text{-}FITC}$ /S (1/μm^2)	3 ± 8	161 ± 30	2110 ± 1015	13.1 (5.7–23.8)

*) Mean values ± confidence intervals ($p<0.05$). $N_{FX\text{-}FITC}$ is the mean number of bound factor X molecules. §) Ratios of the mean values; the possible range of values is given in the parentheses.

Table 2: Parameters of factor X binding to platelets and PMPs.

shown in Figure 2. Table 1 presents an estimation of mean fluorescence intensity per surface area unit of an activated platelet and a PMP. To estimate surface area of activated platelets and microparticles, we used the calculated above diameters of activated platelets and PMPs (2.81 and 0.29 μm, respectively). Although the mean fluorescence intensity of a single PMP was lower than that of a single platelet (Fig. 2), the mean fluorescence intensity per membrane surface area unit for PMPs exceeded that for platelets three- to eight-fold depending on the marker.

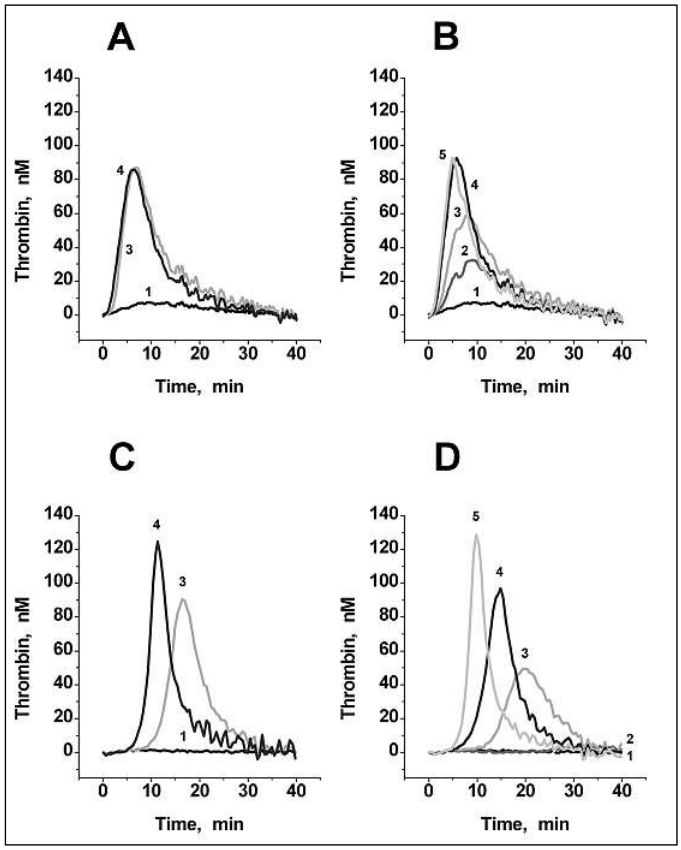

Figure 3: Thrombin generation curves in typical experiment. UFP was supplemented with different concentrations of activated platelets (A, C) or PMPs (B, D). Coagulation was initiated with thromboplastin (A, B) or with kaolin (C, D). For each sample, 90 μl UFP, 10 μl cells/particles suspension and 20 μl of fluorogenic substrate (initial concentration 5 mM) were incubated for 10 min at 37°C. After that, 25 μl of activator was added, and increase of AMC fluorescence was determined on the microplate reader for 40 min. The final concentrations of activators were 4 pM for tissue factor and 0.2 mg/ml for kaolin. Concentrations of added cells/particles for different curves are: (1), 0; (2), 1,760; (3), 17,600; (4), 176,000; (5), 880,000 1/μl.

Calculation of the mean specific fluorescence intensity from the mean fluorescence intensity and the mean diameters might yield inaccurate results for large and asymmetric distributions, because a ratio of two mean values can significantly differ from their mean ratio. Therefore, as controls, we additionally calculated distributions of events by the bound markers or factor X surface densities for our experiments according to formula 2. The mean value of the density distribution did not differ from the value calculated using the means of FSC and fluorescence by more than 10–20%. This is illustrated in Figure 1B showing a normalized distribution of bound factor X density for activated platelets. The mean value of this distribution is 344 arb. un. (CV=66). Calculations using formula 2 and mean values of factor X fluorescence and forward scatter give a value of 287 arb. un. Thus, the difference between the mean density and mean ratio of factor concentration and surface is only 16%. This shows that mean diameters and fluorescence intensities can be used to compare densities of bound ligands.

Determination of factor X binding to the platelet and PMP membranes

To characterize interaction of coagulation factors with platelet and PMP membranes under physiological conditions, binding of FITC-labeled factor X to intact platelets, activated platelets and PMPs was studied by flow cytometry. This parameter was chosen, because factor X binding and activation on procoagulant membranes are critical for the formation and functioning of active tenase and prothrombinase. The experiments were performed at physiological factor X concentration (180 nM). Mean numbers of bound factor X molecules obtained in these experiments are shown in Table 2. There was almost no calcium-dependent factor X binding to intact platelets (52 ± 160 molecules per platelet), while there was significant binding to both activated platelets (3229 ± 606 molecules per platelet) and PMPs (422 ± 203 molecules per platelet). Calculations of the bound factor X mean surface density showed that this density was ~13-fold higher for PMPs than for activated platelets.

As additional controls, we performed experiments to study not only calcium-dependent, but also specific factor X binding. For this purpose, factor X was displaced from its specific sites with excess unlabeled factor X. Potential effect of plasma proteins on this binding was estimated by addition of prothrombin at plasma concentration (1400 nM), which was known as the principal competitor for factor X binding sites (32). For both activated platelets and microparticles, specific factor X binding constituted ~40–50% of calcium-dependent binding, and prothrombin displaced factor X from ~30–40% of its calcium-dependent binding sites (data not shown). Independently of the parameter

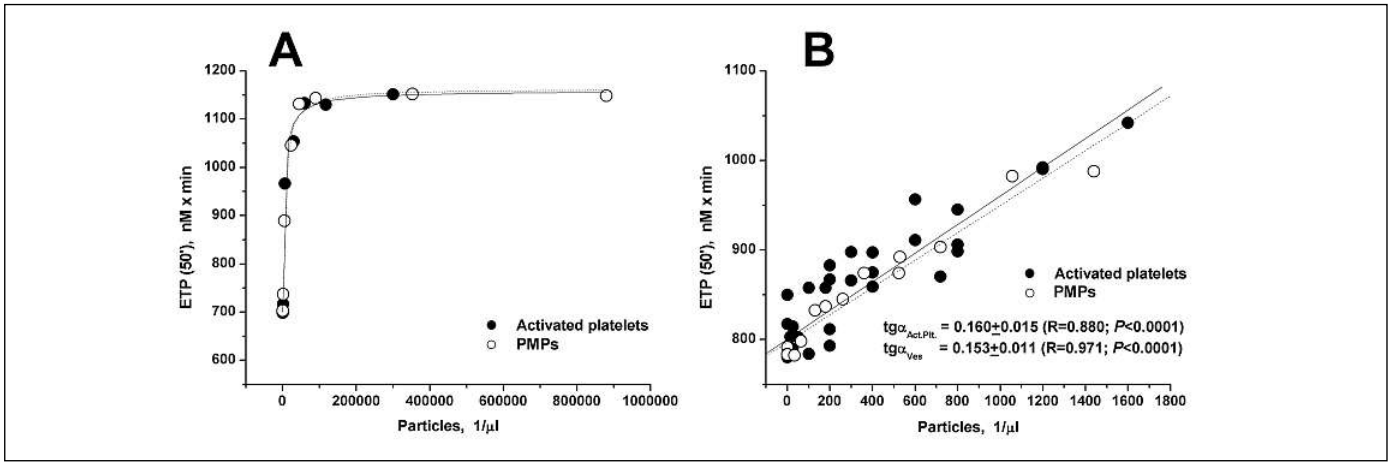

Figure 4: Dependence of endogenous thrombin potential on the concentration of (●) activated platelets, or (○) PMPs added to UFP. Results of a typical experiment (A) and independent experiments for initial sections of the curves for activated platelets (n=5) and PMPs (n=3) (B) are shown. Coagulation was initiated by thromboplastin (4 pM). All conditions were as described in the legend to Figure 3.

chosen to characterize factor X-dependent procoagulant activity, the relation between activated platelets and PMPs was the same.

Parameters of thrombin generation in UFP supplemented with activated platelets or PMPs

Thrombin generation test was used to compare procoagulant activities of platelets and PMPs. Figure 3 presents typical thrombin generation curves obtained upon addition of activated platelets (A, C) or PMPs (B, D) at different concentrations to UFP. Coagulation was activated either via the extrinsic (A, B) or the intrinsic (C, D) pathway. In all cases, the maximal thrombin concentration and the area under the thrombin generation curve rapidly increased with the increase of the concentration of cells/particles added. The maximal possible ETP achieved was also the same for all panels. The initiation phase (time between the beginning of the experiment and the burst of thrombin generation) was shortened with the increase of phospholipid surface. This effect was more pronounced for the kaolin-activated thrombin generation than for the tissue-factor-activated one. Similar results were obtained upon addition of platelets or PMPs to PFP instead of UFP (data not shown).

Figure 4A presents values of ETP obtained in a typical experiment with thromboplastin-activated UFP supplemented with different concentrations of activated platelets or PMPs. Identical results were obtained for kaolin-activated thrombin generation (not shown). There was apparent similarity between the curves for activated platelets and PMPs. With the increase of their concentration, ETP initially increased, followed by a plateau. The plateau level was almost the same for activated platelets and PMPs. Control experiments with PRP and frozen/thawed PRP confirmed that this maximum was the true maximum determined not by the quantity or type of lipid surface but by the inner

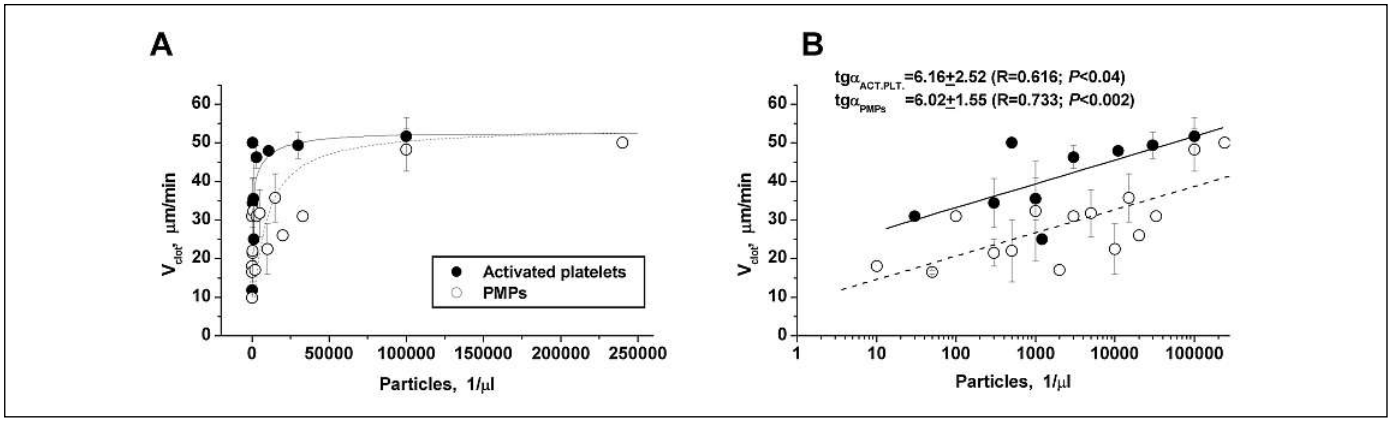

Figure 5: The rate of spatial clot growth in UFP as a function of the concentration of added (●) activated platelets, or (○) PMPs in linear (A) and semi-logarithmic (B) scales. Mean values ± SD are shown, n=1–7. UFP (500 μl) was supplemented with 10 μl of the suspension of analyzed cells/particles (final concentrations are indicated in the figure) and recalcified by the addition of 10 μl of 1 M $CaCl_2$ solution. V_{clot} was studied at 37°C in a microchamber, where one wall was covered with a film with tissue-factor expressing fibroblasts. Spatial distribution of the light scatter was recorded each 30 seconds with a video camera. V_{clot} was determined from the obtained light scattering profiles as described in the *Materials and methods*.

properties of the plasma coagulation system. Figure 4B shows the results of the linear approximations of the initial portions of these dependences (summarized for all experiments). They indicate that the procoagulant activity of a single PMP is almost equal to that of an activated platelet.

Spatial clot growth rate in the presence of activated platelets or PMPs

The effect of activated platelets and PMPs on the propagation of coagulation was studied in a reaction-diffusion model of clot formation. A typical dependence of V_{clot} on the concentration of platelets or PMPs added to UFP was a steep curve with rapid saturation similar to those observed in thrombin generation model (Fig. 5A). The plateau value (maximal spatial clot growth rate) was the same for all types of supplemented cells/particles. Figure 5B displays averaged results of all experiments on clot formation in UFP supplemented with activated platelets or PMPs. For better presentation, results are shown in semi-logarithmic scale. The dependence followed a logarithmic law within a wide range of concentrations. The slopes of the lines in a semi-logarithmic scale for activated platelets and PMPs were almost identical: 6.16 ± 2.52 ($R=0.678$, $p<0.04$) and 6.02 ± 1.55 ($R=0.733$, $p<0.002$), respectively.

Discussion

Our in-vitro comparison of procoagulant properties of activated platelets and PMPs showed that the surface of PMPs was at least 50- to 100-fold more procoagulant. This effect was demonstrated by determination of thrombin generation and spatial clot growth parameters in UFP supplemented with different concentrations of activated platelets or PMPs. Control experiments confirmed that concentration of phospholipid surfaces essential for the assembly of procoagulant complexes was significantly reduced in UFP.

Platelets and PMPs were characterized by flow cytometry. For intact platelets, binding of the PS marker annexin V-FITC (14) and anti-CD62P-PE was almost undetectable. Both signals were greatly increased in activated platelets (Fig. 2). They were also always present on the membranes of PMPs. Although mean fluorescence intensity of these markers per event was higher for activated platelets than for PMPs, platelets are much larger than PMPs. To compare specific membrane activities, we estimated the fluorescence per surface area unit for platelets and PMPs. Mean diameters of activated platelets and PMPs in our experiments were calculated from FSC using a calibration curve prepared with size calibration beads of different diameters. The obtained mean diameters of activated platelets and PMPs were 2.81 and 0.29 μm, respectively. This is in agreement with the data of another study (33), where FSC distribution of particles in plasma was compared with FSC distributions for the mixtures of calibrated synthetic phospholipid vesicles. According to that study, most particles in plasma had a diameter of 0.25 μm, while the diameter of 0.4 μm was on the right boundary of the distribution. Mean fluorescence intensities per surface area unit of platelets and PMPs (Table 1) showed that PMP membranes were enriched with PS, general, and activation platelet markers. These results would remain valid if the PMP surface was estimated using diameter up to 0.4 μm. If we took into consideration that PMP diameter can be smaller than 0.29 μm, the enrichment effect on vesicles would become even more pronounced. A similar increase in numbers of calcium-dependent factor X binding sites per surface unit for PMPs in comparison with activated platelets was observed when factor X was added to suspensions of washed cells/particles at the physiological concentration of 180 nM (Table 2).

These results agree with the reports indicating that PMP membranes become enriched with different receptors and, probably, with PS during vesiculation (13–16, 34). However, although those studies suggested a significant role for PMPs in the coagulation process, they did not show it directly. There is a complex non-linear relation between the density of a bound factor and the rate of a membrane-dependent reaction. Interactions between plasma proteins can also significantly change estimations obtained in purified systems. Moreover, rates of individual reactions are not directly related to the global response of the coagulation system. Of note, significant enrichment was not observed for all receptors. In contrast to factors Va and VIII (15, 16), factor IXa binding sites were concentrated on PMPs only to a very small degree (34). Finally, PMPs were shown to efficiently accelerate not only the pro-coagulant reactions, but also the anti-coagulant ones (17). Therefore, the binding data alone did not allow estimation of the procoagulant role of PMPs. That is why the present work uses not only flow cytometry data, but also plasma-based in-vitro clotting models to compare procoagulant activities of activated platelet and PMP membranes.

Previous studies of thrombin generation (9–12) were performed for short time periods. Only initial parts of thrombin generation curves were obtained. They reported that clotting was somewhat accelerated by the presence of PMPs. These short experiments did not allow determination of the total thrombin produced. A recent work by Keuren et al. (35) investigated the effect of storage-induced PMPs on thrombin and factor X generation. It demonstrated that these PMPs not only increased thrombin generation, but also resulted in a 15-fold higher maximal thrombin generation rate than synthetic phospholipid vesicles. However, the authors point out that storage-induced PMPs can have properties dramatically different from those formed during platelet activation. Finally, none of these studies compared activity of PMPs with that of activated platelets.

Thrombin generation curves obtained in our study (Fig. 3) provide evidence that the increase of activated platelets or PMP concentration accelerates the onset of coagulation and increases maximal thrombin concentration. The total thrombin produced (ETP) was also increased (Fig. 4A). These results did not depend qualitatively on the initiation pathway of coagulation (Fig. 3). The most intriguing, however, is not the acceleration and the increase of thrombin generation, which could be expected, but the fact that increases of ETP per one platelet or PMP added were not significantly different. This result is illustrated by Figure 4B, where more detailed initial sections of ETP-dependences on the particle/cell concentrations are shown. These initial sections could be approximated with the lines of similar slopes: 0.160 ± 0.015 for activated platelets, and 0.153 ± 0.011 for PMPs.

Determination of clot growth rate in UFP supplemented with activated platelets and PMPs gave similar results. The data in

Figure 5 show dose-dependent acceleration of clotting in UFP upon supplementation with different particles. The same plateau value of V_{clot} for both types of plasma supplementation suggests that this level is determined not by the type of added particles, but by the properties of plasma. Results for activated platelets and PMPs in Figure 5 are similar. The obtained curves are presented in a semi-logarithmic scale and are approximated with lines (Fig. 5B). The slopes of these lines for activated platelets and PMPs were nearly the same (6.16 ± 2.52 and 6.02 ± 1.55, respectively).

Thus, if procoagulant activity of a single activated platelet is almost identical to that of a single PMP, and two PMP are shed per one A23187-activated platelet (13), these PMPs should provide a total procoagulant activity even somewhat exceeding that of an activated platelet itself. This is indeed the case, as has been reported (36). On the other hand, the surface of a PMP is about 100-fold smaller than that of a platelet (0.26 and 24.8 μm^2, respectively, assuming PMP diameter to be 0.29 μm). Therefore, the procoagulant activity of a PMP per surface area unit is almost 50- to 100-fold higher than appropriate activity of an activated platelet. This effect will only increase if particle size is actually less than 0.29 μm.

There was an interesting difference between various tests determining specific procoagulant activity of PMPs and activated platelets. Phosphatidylserine expression, factor X binding, and thrombin generation in plasma gave values of three-, 13-, and 50- to 100-fold difference in the activity per surface unit, respectively. The most probable reason for this discrepancy is difference in PMP-membrane concentrations of other membrane components. The principal candidates for this role are proteins. Previous studies (13–16, 34) have shown the possibility of such membrane receptor enrichment. Recent work (35) also suggests that phosphatidylserine is not the only determinant of the vesicle procoagulant activity. The difference between enhancement of factor X binding per surface area unit and of thrombin generation (13-fold and 50-fold, respectively) suggests that PMPs efficiently accelerate not only the factor X-involving reactions, but also other processes, which in summary leads to the potent procoagulant effect.

In our experiments, the summary procoagulant effect of PMP membranes was several-fold lower then in (15, 16). This difference can be explained by our assays having been performed in plasma containing normal levels of coagulation factors and inhibitors. Anticoagulant properties of PMPs, such as acceleration of prothrombinase inhibition on the PMP surface (17), should also contribute to their overall effect. In addition, as discussed above, the relative activity of PMPs with respect to activated platelets can only increase if the diameter of PMP is smaller than the estimation in our study. For PMPs with the diameter of 0.1 μm this value would be 300- to 600-fold.

Summarizing, the data obtained in this study show that, under normal conditions, a surface area unit of a PMP has at least approximately 50- to 100-fold higher procoagulant properties than an identical surface area unit of an activated platelet. This is a result not only of increased procoagulant phospholipids density, but also of the increased density of receptors for the procoagulant complexes assembly. Small active PMPs can easily be carried by blood flow far away from the initial site of coagulation initiation. This can potentially lead to dangerous thrombosis.

Stimulation with calcium ionopore A23187 was chosen in this study as a simple, well-established and well-characterized model of platelet activation. This model does not include physiological processes of the first activation stages (leading to the increase of intracellular calcium), but focuses instead on the consequences caused by this increase. These consequences should be qualitatively independent of the specific reason of calcium concentration increase. However, quantitative parameters of the process would obviously depend on the type of activator used. Therefore, further investigation of the conclusions of this study with various combinations of physiological and pathophysiological activators appears to be interesting and important.

Acknowledgements

We thank Dr. L. I. Ul'yanova (Institute of Immunology, Moscow, Russia) for assistance with fibroblast culture. We are deeply grateful to V. D. Afanas'eva (National Research Center for Hematology) for her kind help with blood collection.

References

1. Schenone M, Furie BC, Furie B. The blood coagulation cascade. Curr Opin Hematol 2004; 11: 272–277.

2. Bevers EM, Comfurius P, Dekkers DW, et al. Lipid translocation across the membrane of mammalian cells. Biochim Biophys Acta 1999; 1439: 317–330.

3. Kalafatis M, Swords NA, Rand MD, et al. Membrane-dependent reactions in blood coagulation: role of the vitamin K-dependent enzyme complexes. Biochim Biophys Acta 1994; 1227: 113–129.

4. Horstman LL, Ahn YS. Platelet microparticles: a wide-angle perspective. Platelet microparticles: a wide-angle perspective. Crit Rev Oncol Hematol 1999; 30: 111–142.

5. Freyssinet JM. Cellular microparticles: what are they bad or good for? J Thromb Haemost 2003; 1: 1655–1662.

6. Morel O, Toti F, Hugel B, et al. Cellular microparticles: a disseminated storage pool of bioactive vascular effectors. Curr Opin Hematol 2004; 11: 156–164.

7. Ahn YS. Cell-derived microparticles: 'Miniature envoys with many faces'. J Thromb Haemost 2005; 3: 884–887.

8. Horstman LL, Jy W, Junenez JJ, et al. New horizons in the analysis of circulating cell-derived microparticles. Keio J Med 2004; 53: 210–230.

9. Nieuwland R, Berckmans RJ, Rotteveel-Eijkman RC, et al. Cell-derived microparticles generated in patients during cardiopulmonary bypass is highly procoagulant. Circulation 1997; 96: 3534–3541.

10. Nieuwland R, Berckmans RJ, McGregor S, et al. Cellular origin and procoagulant properties of microparticles in meningococcal sepsis. Blood 2000; 95: 930–935.

11. Joop K, Berckmans RJ, Nieuwland R, et al. Microparticles from patients with multiple organ dysfunction syndrome and sepsis support coagulation through multiple mechanisms. Thromb Haemost 2001; 85: 810–820.

12. Berckmans RJ, Nieuwland R, Böing AN, et al. Cell-derived microparticles circulate in healthy humans and support low grade thrombin generation. Thromb Haemost 2001; 85: 639–646.

13. Sims PJ, Wiedmer T, Esmon CT, et al. Assembly of platelet prothrombinase complex is linked to vesiculation of platelet plasma membrane. Studies in Scott syndrome: an isolated defect in platelet procoagulant activity. J Biol Chem 1989; 264: 17049–17057.

14. Dechary-Prigent J, Freyssinet JM, Pasquet JM, et al. Annexin V as a probe of aminophospholipid exposure and platelet membrane vesiculation: a flow cytometry study showing a role for free sulfhydryl groups. Blood 1993; 81: 2554–2565.

15. Sims PJ, Faioni EM, Wiedmer T, et al. Complement proteins C5b-9 cause release of membrane vesicles from the platelet surface that are enriched in the membrane receptor for coagulation factor Va and express prothrombinase activity. J Biol Chem 1988; 263: 18205–18212.

16. Gilbert GE, Sims PJ, Wiedmer T, et al. Platelet-derived microparticles express high affinity receptors for factor VIII. J Biol Chem 1991; 266: 17261–17268.
17. Tans G, Rosing J, Tomassen MCLGD, et al. Comparison of anticoagulant and procoagulant activities of stimulated platelets and platelet-derived microparticles. Blood 1991; 77: 2641–2648.
18. Hemker HC, Giesen PL, Ramjee M, et al. The thrombogram: monitoring thrombin generation in platelet-rich plasma. Thromb Haemost 2000; 83: 589–591.
19. Ovanesov MV, Krasotkina JV, Ul'yanova LI, et al. Hemophilia A and B are associated with abnormal spatial dynamics of clot growth. Biochim Biophys Acta 2002; 1572: 45–57.
20. Ovanesov MV, Lopatina EG, Saenko EL, et al. Effect of factor VIII on tissue factor-initiated spatial clot growth. Thromb Haemost 2003; 89: 235–242.
21. Ovanesov MV, Ananyeva NM, Panteleev MA, et al. Initiation and propagation of coagulation from tissue factor-bearing cell monolayers to plasma: initiator cells do not regulate spatial growth rate. J Thromb Haemost 2005; 3: 321–331.
22. Kawabata S, Miura T, Morita T, et al. Highly sensitive peptide-4-methylcoumaryl-7-amide substrates for blood-clotting proteases and trypsin. Eur J Biochem 1988; 172: 17–25.
23. Sinauridze EI, Volkova RI, Krasotkina YV, et al. Dynamics of clot growth induced by thrombin diffusing into nonstirred citrate human plasma. Biochim Biophys Acta 1998; 1425: 607–616.
24. Korotina NG, Ovanesov MV, Plyushch OP, et al. Study of the spontaneous clots in normal plasma and plasma of haemophilia A patients. Gematol Transfuziol, 2002; 47: 26–29.
25. Taube J, McWilliam N, Luddington R, et al. Activated protein C resistance: effect of platelet activation, platelet-derived microparticles, and atherogenic lipoproteins. Blood 1999; 93: 3792–3797.
26. Freifelder D. Sedimentation. In: Physical Biochemistry. Applications to Biochemistry and Molecular Biology, Part IV (Hydrodinamic Methods), WH Freeman and Company, San Francisco, 1976, p. 275–349.
27. Panteleev MA, Ananyeva NM, Greco NJ, et al. Two subpopulations of thrombin-activated platelets differ in their binding of the components of the intrinsic factor X-activating complex. J Thromb Haemost 2005; 3: 2545–2553.
28. Barry OP, Kazanietz MG, Pratico D, et al. Arachidonic acid in platelet microparticles up-regulates cyclooxygenase-2-dependent prostaglandin formation via a protein kinase C/mitogen-activated protein kinase-dependent pathway. J Biol Chem 1999; 274: 7545–7556.
29. Vidal C, Spaulding C, Picard F, et al. Flow cytometry detection of platelet procoagulant activity and microparticles in patients with unstable angina treated by percutaneous coronary angioplasty and stent implantation. Thromb Haemost 2001; 86: 784–790.
30. Michelson AD, Barnard MR, Krueger LA, et al. Evaluation of platelet function by flow cytometry. Methods 2000; 21: 259–270.
31. Sinha D, Seaman FS, Koshy A, et al. Blood coagulation factor XIa binds specifically to a site on activated human platelets distinct from that for factor XI. J Clin Invest 1984; 73: 1550–1556.
32. Scandura JM, Ahmad SS, Walsh PN. A binding site expressed on the surface of activated human platelets is shared by factor X and prothrombin. Biochemistry 1996; 35: 8890–8902.
33. Muller I, Klocke A, Alex M, et al. Intravascular tissue factor initiates coagulation via circulating microvesicles and platelets. FASEB J 2003; 17: 476–488.
34. Hoffman M, Monroe DM, Roberts HR. Coagulation factor IXa binding to activated platelets and platelet-derived microparticles: a flow cytometric study. Thromb Haemost 1992; 68: 74–78.
35. Keuren JF, Magdeleyns EJ, Govers-Riemslag JW, et al. Effects of storage-induced platelet microparticles on the initiation and propagation phase of blood coagulation. Br J Haematol 2006; 134: 307–313.
36. Fox JE, Austin CD, Reynolds CC, et al. Evidence that agonist-induced activation of calpain causes the shedding of procoagulant-containing microvesicles from the membrane of aggregating platelets. J Biol Chem 1991; 266: 13289–13295.